J|A|C|S COMMUNICATIONS

Published on Web 09/13/2010

Post-Synthesis Carbon Doping of Individual Multiwalled Boron Nitride Nanotubes via Electron-Beam Irradiation

Xianlong Wei,* Ming-Sheng Wang, Yoshio Bando, and Dmitri Golberg*

International Center for Materials Nanoarchitectonics (MANA), National Institute for Materials Science (NIMS), Namiki 1-1, Tsukuba, Ibaraki 305-0044, Japan

Received July 12, 2010; E-mail: weixl@pku.edu.cn; GOLBERG.Dmitri@nims.go.jp

Abstract: We report on post-synthesis carbon doping of individual boron nitride nanotubes (BNNTs) via in situ electron-beam irradiation inside an energy-filtering 300 keV high-resolution transmission electron microscope. The substitution of C for B and N atoms in the honeycomb lattice was demonstrated through electron energy loss spectroscopy, spatially resolved energy-filtered elemental mapping, and in situ electrical measurements. Substitutional C doping transformed BNNTs from electrical insulators to conductors. In comparison with the existing post-synthesis doping methods for nanoscale materials (e.g., ion implantation and diffusion), the discovered electron-beam-induced doping is a well-controlled, little-damaging, room-temperature, and simple strategy that is expected to demonstrate great promise for post-synthesis doping of diverse nanomaterials in the future.

Well-controlled doping aimed at tailoring electrical, optical, and magnetic properties for specific applications is a highly important topic in "bottom-up" nanoscale materials research. In comparison with most doping events, which occur by dopant introduction during synthesis,[1] post-synthesis doping could place specific dopants into well-defined regions through masking/lithography after nanomaterial synthesis and even at the stage of device fabrication,[2b,3b] as has been demonstrated utilizing ion implantation[2] and diffusion.[3] However, post-synthesis doping still suffers from severe crystal damage under ion implantation,[2] the high temperatures needed for diffusion,[3] and the complex procedures involved in masking[2b] and lithography[3b] to define doping regions or in introducing dopants.[3a] Herein, we report on the post-synthesis carbon doping of individual multiwalled boron nitride nanotubes (BNNTs) via a well-controlled, mild-conditions, room-temperature, and simple strategy based on in situ electron-beam irradiation of the tube in a transmission electron microscope (TEM).

BNNTs, a structural equivalent of carbon nanotubes (CNTs), exhibit rival mechanical properties and considerably higher thermal and chemical stabilities than CNTs.[4a] In contrast to the uncontrollable chirality-dependent electrical properties of their C counterparts, BNNTs are electrical insulators with a helicity-independent band gap of ~5.5 eV.[4,5] As hybrids of BNNTs and CNTs, ternary B−C−N nanotubes exhibit tunable electrical properties intermediate between those of BNNTs and CNTs that depend on relative elemental fractions and spatial arrangements of the elements.[4c,6] Therefore, well-controlled C doping of BNNTs offers the rare possibility of delicate tailoring of the electrical properties of a nanotube. Even though B−C−N nanotubes have been synthesized by doping CNTs with B and N[1a,4a,c,6b] and obtained by C doping of BNNTs through diffusion,[6d] post-synthesis C doping of BNNTs providing well-defined doped regions and well-controlled dopant concentrations remains a grand challenge.

The in situ experiments were performed at room temperature inside a 300 kV JEOL 3100FEF (Omega Filter) field-emission high-resolution TEM (HRTEM) equipped with a scanning tunneling microscope (STM)−TEM "Nanofactory Instruments" holder. High-purity BNNTs synthesized by a chemical vapor deposition method were used (Figure S1 in the Supporting Information).[7] For C doping, a tiny amount of paraffin wax (C_nH_{2n+2} with $19 \leq n \leq 36$) was placed several millimeters away from the mounted BNNT samples (Figure S2), and then the BNNT selected for doping was irradiated with an electron beam. The introduction of paraffin wax induced the absorption of hydrocarbon molecules on the surface of BNNTs.[8a] Under electron-beam irradiation, C species appeared as a result of decomposition of the hydrocarbon molecules.[8] Herein, we show that the decomposed C can be substituted for B or N atoms within the tube lattice when the tube is bombarded with high-energy electrons (Figure 1a). To thoroughly confirm substitutional C doping of BNNTs, structure and composition characterizations and in-tandem electrical measurements were performed on the same tube before and after doping. We obtained similar results from 13 individual BNNTs. In order to provide a fully consistent, complete, and detailed picture, the data presented in this communication were collected from the same tube.

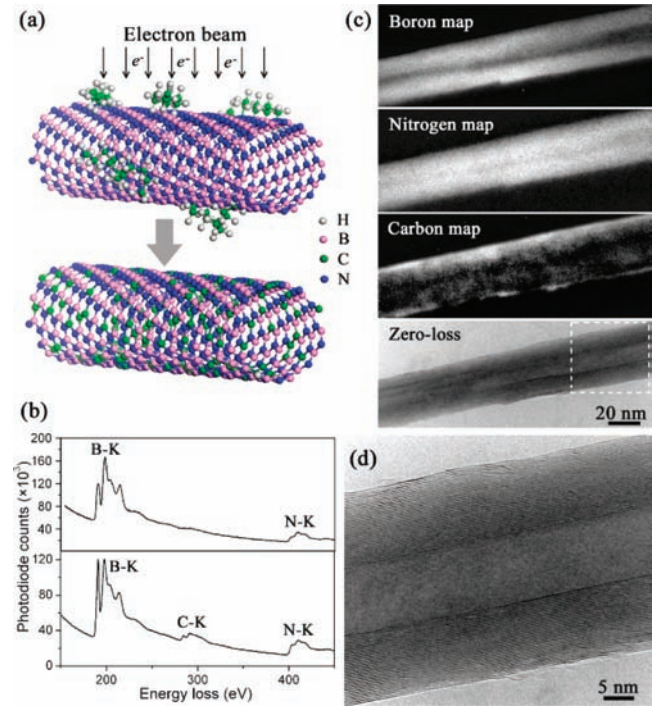

Figure 1. (a) Schematic drawing of electron-beam-induced C doping of a BNNT. (b) EEL spectra of the BNNT in the beginning (top) and end (bottom) of C doping. (c) Zero-loss and corresponding spatially resolved elemental maps of the BNNT after doping. (d) HRTEM image of the framed area in the zero-loss image in (c).

Figure 1b shows electron energy loss (EEL) spectra of the same BNNT acquired in the beginning and end of C doping. The characteristic K-edges of B at 188 eV and N at 401 eV are clearly identified.

 10.1021/ja106134s

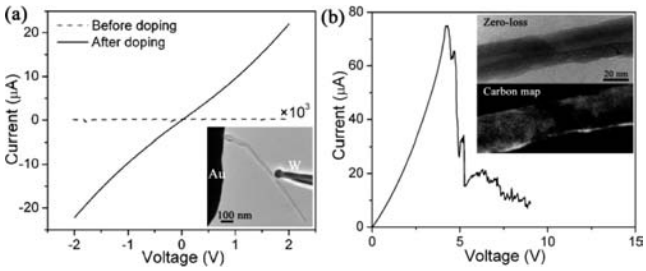

Figure 2. a) Two-terminal $I-V$ curves of a BNNT before and after C doping. The inset is a TEM image showing how the tube was connected to gold and tungsten electrodes. (b) $I-V$ curve measured during tube thinning under electrical current flow. The inset shows zero-loss and C elemental maps after thinning.

In contrast to the EEL spectrum showing a negligible C content (~2 atom %) in the beginning of doping, the characteristic K-edge of C appeared at 284 eV with sharp π^* and σ^* peaks after doping. This indicates that sp^2-hybridized C was incorporated into the BNNT. Quantification of the EEL spectrum after doping gave a B/C/N atomic ratio of 0.77:0.25:1.00, indicating that C seems to preferentially substitute for B atoms in the honeycomb lattice (Figure S3). The incorporation of C was also confirmed by spatially resolved elemental maps (Figure 1c). Almost the same intensity profiles were obtained from B, N, and C maps (Figure S4). The C map showed a higher C concentration in the outer shells, where C doping was initiated. An HRTEM image of the tube (Figure 1d) showed well-structured tubular shells after doping, providing solid evidence that the present electron-beam-induced doping occurs within the tube lattice under little-damage conditions. The absence of a separate C-layer coating on the BNNT in Figure 1d, the nearly identical intensity profiles in the B, N, and C maps, the unequal atomic percentages of B and N, and the absence of a diameter increase as a result of doping (Figure S5) enable us to unambiguously conclude that C was incorporated by substitution for B or N atoms in the honeycomb tube network but not through formation of a surface C shield.

The substitutional C doping of the BNNT was further confirmed by direct electrical measurements. The tube was electrically insulating with no detectable current under a bias voltage of 10 V before doping, in agreement with the previous measurements on pure BNNTs.[9] Once the tube was irradiated with electrons in the presence of paraffin wax droplets in its vicinity, its conductance dramatically increased and kept increasing with irradiation time (Figure S6). The tube finally became metallic with a measured resistance as low as ~90 kΩ (Figure 2a). The conductance increase with irradiation time is attributed to an increase in C content,[6b] so the C concentration, and thus the electrical properties of BNNTs, can be engineered by a simple irradiation time control. In order to visualize tube failure, the bias voltage was gradually increased until a steep current decrease appeared (Figure 2b). However, at this stage, the tube had not completely failed but was only thinned by ~6 nm in its middle portion (Figure S5). Repeatedly acquired elemental maps showed the appearance of a gap in the C map at the thinned portion but not in the B and N maps (Figure 2b inset and Figure S7). This definitely indicates that the current of the tube was mainly carried by the outer C-doped BNNT shells. In other words, C doping of the outer shells changed the BNNT from an insulator to a conductor.

The knock-out ejections of B and N atoms and subsequent healing of vacancy defects with C atoms are proposed to be responsible for the discovered electron-beam-induced doping. Threshold electron-beam energies for B and N atom ejections from BNNTs were found to be ~80 keV[10a,b] (79.5 and 118.6 keV in the most recent publication[10c]); these are much lower than the working voltage of 300 keV in our experiments. Since the formation energies of substitutional C defects at both B and N sites have been predicted to be lower than those of B and N vacancies,[11] the B and N vacancies produced by knock-out ejection would immediately be filled by C atoms originated from decomposed hydrocarbon molecules.

To sum up, substitutional C doping of individual multiwalled BNNTs was achieved in situ inside an HRTEM via electron-beam irradiation, resulting in the transformation of the BNNTs from electrical insulators to conductors. Since the electron beam can be focused down to a subnanometer size and be well-controlled in a manner peculiar to electron-beam lithography, the presently discovered electron-beam-induced doping is expected to produce well-defined doped regions with subnanometer resolution. Furthermore, the dopant concentration can be perfectly controlled through tuning of the irradiation time and beam energy. Apart from individual BNNTs, simultaneous doping of large fractions of nanotube powders can also be achieved using irradiation of correspondingly larger areas. The reported process is envisaged to be a promising method for on-demand doping of a given nanomaterial in the future as a consequence of its perfect controllability, relative simplicity, minor-damaging, and room temperature conditions.

Acknowledgment. This work was supported by the International Center for Materials Nanoarchitectonics (MANA) of the National Institute for Materials Science (NIMS).

Supporting Information Available: Experimental details, elemental contents in doped BNNTs, cross-sectional tube profiles in spatially resolved elemental maps, tube diameter comparisons before and after doping and thinning, electrical measurements during doping, spatially resolved elemental maps, and tube structures after thinning. This material is available free of charge via the Internet at http://pubs.acs.org.

References

(1) (a) Stephan, O.; Ajayan, P. M.; Colliex, C.; Redlich, P.; Lambert, J. M.; Bernier, P.; Lefin, P. *Science* **1994**, *266*, 1683. (b) Golberg, D.; Bando, Y.; Bourgeois, L.; Kurashima, K.; Sato, T. *Carbon* **2000**, *38*, 2017. (c) Wang, Y.; Lew, K.-K.; Ho, T.-T.; Pan, L.; Novak, S. W.; Dickey, E. C.; Redwing, J. M.; Mayer, T. S. *Nano Lett.* **2005**, *5*, 2139.
(2) (a) Krasheninnikov, A. V.; Nordlund, K. *J. Appl. Phys.* **2010**, *107*, 071301and references therein. (b) Hoffmann, S.; Bauer, J.; Ronning, C.; Stelzner, T.; Michler, J.; Ballif, C.; Sivakov, V.; Christiansen, S. H. *Nano Lett.* **2009**, *9*, 1341. (c) Bangert, U.; Bleloch, A.; Gass, M. H.; Seepujak, A.; van der Berg, J. *Phys. Rev. B* **2010**, *81*, 245423. (d) Ghicov, A.; Macak, J. M.; Tsuchiya, H.; Kunze, J.; Haeublein, V.; Frey, L.; Schmuki, P. *Nano Lett.* **2006**, *6*, 1080.
(3) (a) Ho, J. C.; Yerushalmi, R.; Jacobson, Z. A.; Fan, Z. Y.; Alley, R. L.; Javey, A. *Nat. Mater.* **2008**, *7*, 62. (b) Ford, A. C.; Chuang, S.; Ho, J. C.; Chueh, Y.-L.; Fan, Z. Y.; Javey, A. *Nano Lett.* **2010**, *10*, 509. (c) Yim, J. W. L.; Chen, D.; Brown, G. F.; Wu, J. Q. *Nano Res.* **2009**, *2*, 931. (d) Ingole, S.; Aella, P.; Manandhar, P.; Chikkannanavar, S. B.; Akhadov, E. A.; Smith, D. J.; Picraux, S. T. *J. Appl. Phys.* **2008**, *103*, 104302.
(4) (a) Golberg, D.; Bando, Y.; Tang, C. C.; Zhi, C. Y. *Adv. Mater.* **2007**, *19*, 2413, and references therein. (b) Golberg, D.; Bando, Y.; Huang, Y.; Terao, T.; Mitome, M.; Tang, C. C.; Zhi, C. Y. *ACS Nano* **2010**, *4*, 2979, and references therein. (c) Ayala, P.; Arenal, R.; Loiseau, A.; Rubio, A.; Pichler, T. *Rev. Mod. Phys.* **2010**, *82*, 1843, and references therein.
(5) Blase, X.; Rubio, A.; Louie, S. G.; Cohen, M. L. *Europhys. Lett.* **1994**, *28*, 335.
(6) (a) Miyamoto, Y.; Rubio, A.; Cohen, M. L.; Louie, S. G. *Phys. Rev. B* **1994**, *50*, 4976. (b) Golberg, D.; Bando, Y.; Dorozhkin, P.; Dong, Z. C. *MRS Bull.* **2004**, *29*, 38. (c) Mazzoni, M. S. C.; Nunes, R. W.; Azevedo, S.; Chacham, H. *Phys. Rev. B* **2006**, *73*, 073108. (d) Wang, W. L.; Bando, Y.; Zhi, C. Y.; Fu, W. Y.; Wang, E. G.; Golberg, D. *J. Am. Chem. Soc.* **2008**, *130*, 8144.
(7) Tang, C. C.; Bando, Y.; Sato, T.; Kurashima, K. *Chem. Commun.* **2002**, 1290.
(8) (a) Ding, W.; Dikin, D. A.; Chen, X.; Piner, R. D.; Ruoff, R. S.; Zussman, E.; Wang, X.; Li, X. *J. Appl. Phys.* **2005**, *98*, 014905. (b) Van Dorp, W. F.; Hagen, C. W. *J. Appl. Phys.* **2008**, *104*, 081301and references therein.
(9) (a) Cumings, J.; Zettl, A. *Solid State Commun.* **2004**, *129*, 661. (b) Xu, Z.; Golberg, D.; Bando, Y. *Nano Lett.* **2009**, *9*, 2251.
(10) (a) Zobelli, A.; Gloter, A.; Ewels, C. P.; Seifert, G.; Colliex, C. *Phys. Rev. B* **2007**, *75*, 245402. (b) Zobelli, A.; Gloter, A.; Ewels, C. P.; Colliex, C. *Phys. Rev. B* **2008**, *77*, 045410. (c) Kotakoski, J.; Jin, C. H.; Lehtinen, O.; Suenaga, K.; Krasheninnikov, A. V. *Phys. Rev. B* **2010**, *82*, 113404.
(11) Azevedo, S.; Kaschny, J. R.; de Castilho, C. M. C.; de Brito Mota, F. *Nanotechnology* **2007**, *18*, 495707.

JA106134S